Bioimaging **4** (1996) 198–207. Printed in the UK

Multiphoton excitation cross-sections of molecular fluorophores

Chris Xu, R M Williams, Warren Zipfel and Watt W Webb

Department of Applied Physics, Cornell University, Ithaca, NY 14853, USA

Submitted 30 September 1996, accepted 28 November 1996

Abstract. Nonlinear excitation of fluorophores through molecular absorption of two or three near-infra-red photons from the tightly focused femtosecond pulses of a mode-locked laser offers the cellular biologist an unprecedented panoply of biomolecular indicators for microscopic imaging and cellular analysis. Measurements of the two-photon excitation spectra of 25 ultra-violet and visible absorbing fluorophores from 690 to 1050 nm reveal useful cross sections for near infra-red excitation, providing an artist's palette of emission markers, chemical indicators, and native cellular absorbers for living biological preparations. Measurements of three-photon fluorophore excitation spectra now suggest relatively benign wavelengths to excite deeper UV fluorophores. The inherent optical sectioning capabilities of focused nonlinear excitation provides three-dimensional resolution for imaging and avoids out-of-focus background. Measured nonlinear excitation spectra are described and implications to nonlinear microscopy for biological imaging are defined.

Keywords: fluorescence microscopy, multiphoton excitation, cross-sections, fluorophores, 3-D imaging

1. Introduction

In 1931 Maria Göppert-Mayer first predicted that an atom or a molecule could absorb two photons simultaneously in the same quantum event (Göppert-Mayer 1931) . The first experimental evidence of this phenomenon came 30 years later when Kaiser and Garret demonstrated two-photon excitation in a CaF_2:Eu^{2+} crystal (Kaiser and Garrett 1961). Several techniques have been used to determine two-photon excitation cross-sections of various materials in the past two decades (Twarowski and Kliger 1977, Sheik-Bahae *et al* 1990, Hermann and Ducuing 1972). Direct measurement of two-photon absorption cross-sections is usually difficult because only a small fraction of photons is absorbed via the two-photon process. Two-photon fluorescence excitation offers an alternative approach to determining two-photon excitation cross-sections provided that the material is fluorescent and its fluorescence quantum efficiency η is known. Although the fluorescence measurements provide excellent sensitivity, accurate determination of absolute two-photon cross-sections is hampered by the strong dependence of absorption rates on the temporal and spatial coherence of the excitation light (Swofford and McClain 1975, Birge 1983), requiring our development of new procedures (Xu and Webb 1996, Xu *et al* 1995).

Denk *et al* (1990) first succeeded in applying two-photon-excited fluorescence to laser scanning microscopy. Because the excitation rate is proportional to the square of illumination intensity, two-photon laser scanning microscopy (2PLSM) provides intrinsic 3-D resolution without background fluorescence as compared to conventional confocal fluorescence microscopy (Denk *et al* 1990). Two-photon laser scanning microscopy has since become a powerful tool for intrinsic three-dimensional fluorescence imaging (Yuste and Denk 1995, Williams *et al* 1994, Denk *et al* 1995, Svoboda *et al* 1996). This discovery has stimulated new interest in the physics of two-photon excitation. Previously, two-photon spectroscopy had mainly been used to study the electronic structure of excited states in molecules (McClain and Harris 1977), where it can access different excited states because its selection rules are different from those for single-photon absorption. Less effort had been devoted to accurate quantitative studies of common fluorophores widely used in 2PLSM, leading to substantial disagreement amongst published values of two-photon cross-sections (Hermann and Ducuing 1972). The lack of knowledge of two-photon excitation cross-sections and spectra for common fluorophores used in biological studies has been a significant obstacle in the use of 2PLSM. In this paper we review our published data with absolute values of two-photon excitation cross-sections for

0966-9051/96/030198+10$19.50

25 commonly used fluorophores in the Ti:sapphire tuning range from 690 nm to 1050 nm. Detailed methods of obtaining these spectra were reported elsewhere (Xu and Webb 1996, Xu *et al* 1995). Our primary motivation has been to establish a reliable data base of two-photon excitation cross-sections in the visible and near IR for two-photon fluorescence microscopy. However, these data, especially with their wide spectral range, should also be valuable to molecular spectroscopists, particularly as a guide for predicting two-photon excitation spectra.

Recently, three-photon-excited fluorescence has been reported for several fluorescent dyes (Gryczynski *et al* 1995a, b). Three-photon fluorescence images have also been obtained by several research groups (Wokosin *et al* 1995, Hell *et al* 1996, Xu *et al* 1996b) We report in this paper our measurements of three-photon-excited fluorescence from UV fluorophores including the Ca^{2+} indicators fura-2 and indo-1, the DNA stain DAPI, and the fluorescent reagent dansyl hydrazine by excitation at $\lambda \sim 1.0\mu$m. We compare the single-, two- and three-photon fluorescence excitation cross-sections of the fluorophores measured and discuss the resulting features of nonlinear microscopy for biological imaging.

2. Two-photon excitation of fluorophores

Figure 1 summarizes results of measurements of two-photon fluorescence excitation spectra ($\sigma_2(\lambda)$) of several fluorophores and Ca^{2+} indicators in the spectral range 690–1050 nm. For comparison, the tuning ranges of several mode-locked laser sources are also plotted in figure 1. Two-photon excitation cross section measurements of another eight dyes, including fluorescein, rhodamine B, DiI, and excitation ratiometric Ca^{2+} indicator fura 2, are shown in figure 2, with their corresponding single-photon absorption spectra. These spectra show that nonlinear fluorescence microscopy based on two-photon excitation can be expected to work well with most existing fluorophores and many available laser sources. For non-ratiometric Ca^{2+} indicators, such as Ca-Crimson, Ca-Orange and Ca-Green-1, we found that the two-photon excitation spectra of the Ca^{2+}-free and Ca^{2+} bound forms are indistinguishable (figure 3). The ratios of fluorescence intensity for the Ca^{2+}-free to Ca^{2+}-bound forms of these indicators are also comparable to their reported single-photon values.

Green fluorescent proteins (GFPs) have attracted tremendous interest as biological reporters for gene expression (Chalfie *et al* 1994). Images of cultured cells using two-photon-excited GFP fluorescence have been reported recently (Niswender *et al* 1995, Potter *et al* 1996). Wildtype GFP has high UV absorption at 400 nm and relatively low visible absorption at 480 nm. To facilitate the use of GFPs with visible excitation, mutant S65T (replacement of Ser65 with Thr) was engineered to

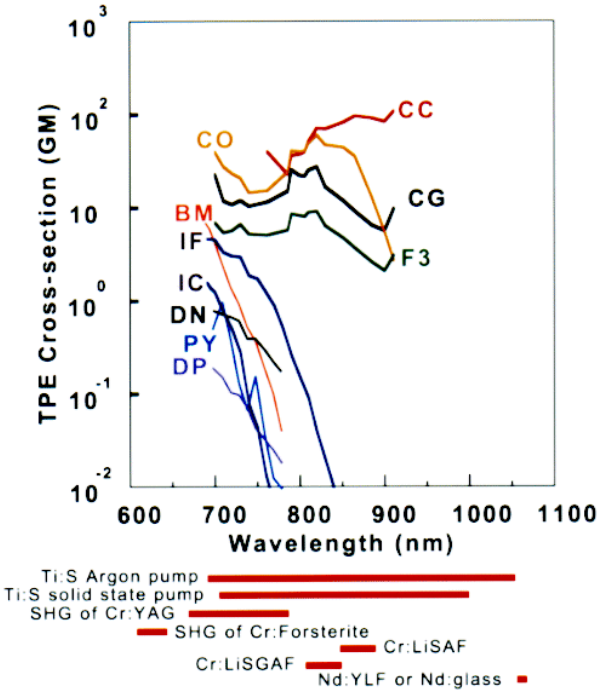

Figure 1. Two-photon fluorescence excitation spectra of fluorophores. For BM(Bis-MSB), the data represent two-photon absorption cross sections. For all the other fluorophores, the data represent two-photon action cross sections, i.e. the product of the fluorescence emission quantum efficiencies and the two-photon absorption cross sections. 1 GM $\equiv 10^{-50}$cm^4 s/photon. Spectra are excited with linearly polarized light using a mode-locked Ti:sapphire laser. For comparison, the tuning range of conveniently available mode-locked laser sources are also plotted. The fluorophores illustrated are: BM $\equiv$ p-bis(*o*-methyl-styryl) benzene. DP (DAPI not DNA bound) $\equiv$ 4′,6-diamidino-2-phenylindole, dyhydrochloride. DN (dansyl) $\equiv$ 5-dimethylaminonaphthalene-1-sulfonyl hydrazine. PY $\equiv$ 1,2-bis-(1-pyrenedecanoyl)-sn-glycero-3-phosphocholine. IC $\equiv$ indo-1 with Ca^{2+}. IF $\equiv$ indo-1 without Ca^{2+}. CG $\equiv$ Calcium green-1 with Ca^{2+}. CO Calcium Orange with Ca^{2+}. CC $\equiv$ Calcium Crimson with Ca^{2+}. F3 $\equiv$ Fluo-3 with Ca^{2+}. All of the samples are purchased from either Eastman Kodak or Molecular Probes. Note that the *y*-axis is in logarithmic scale.

enhance the visible absorption band (Cubitt *et al* 1995). We have measured the two-photon excitation spectra of GFP wildtype and the GFPS65T mutant. Both two-photon excitation spectra are similar to the corresponding single-photon spectra (figure 4). Thus, these results indicate that wildtype GFP can be two-photon excited using the same wavelength needed to excite UV and visible fluorophores (figures 1 and 2), while only long wavelength visible fluorophores can be simultaneously excited with the S65T mutant. The two-photon excitation spectra of another GFP mutant, EGFP (S65T and F64L) (Cormack *et al* 1996) are similar to that of GFPS65T. However, the two-photon excitation fluorescence cross section at 960 nm is approximately 10^2 GM.

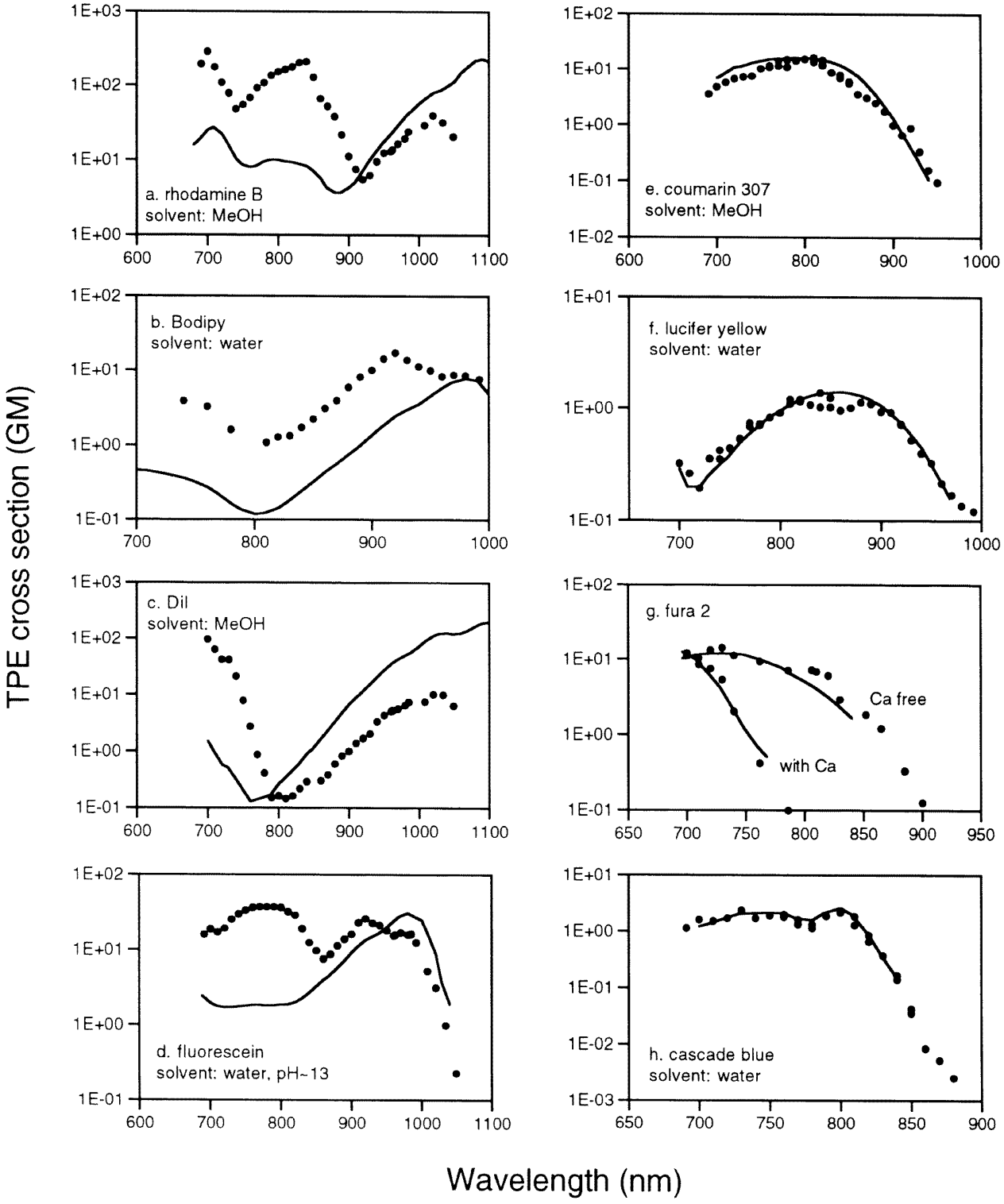

Figure 2. Comparison of single-photon (lines) and two-photon (solid circles) fluorescence excitation spectra. The *y*-axis values represent two-photon action cross sections except for rhodamine B and fluorescein, where values of the two-photon absorption cross sections were given. For the single-photon results, the *x*-axis values represent twice the single-photon transition wavelengths and the *y*-axis values are arbitrarily scaled. DiI (DiI 1,1-dioctadecyl-3,3,3′,3′-tetramethylindocarbocyanine, perchlorate). Cascade Blue ≡ cascade blue hydrazide, trisodium salt. Lucifer Yellow ≡ Lucifer Yellow CH, ammonium salt. Bodipy ≡ 4,4-difluoro-1,3,5,7,8-pentamethyl-4-bora-3a, 4a-diazaindacene-2, 6-disulfonic acid, disodium salt. Note that the *y*-axis is in logarithmic scale.

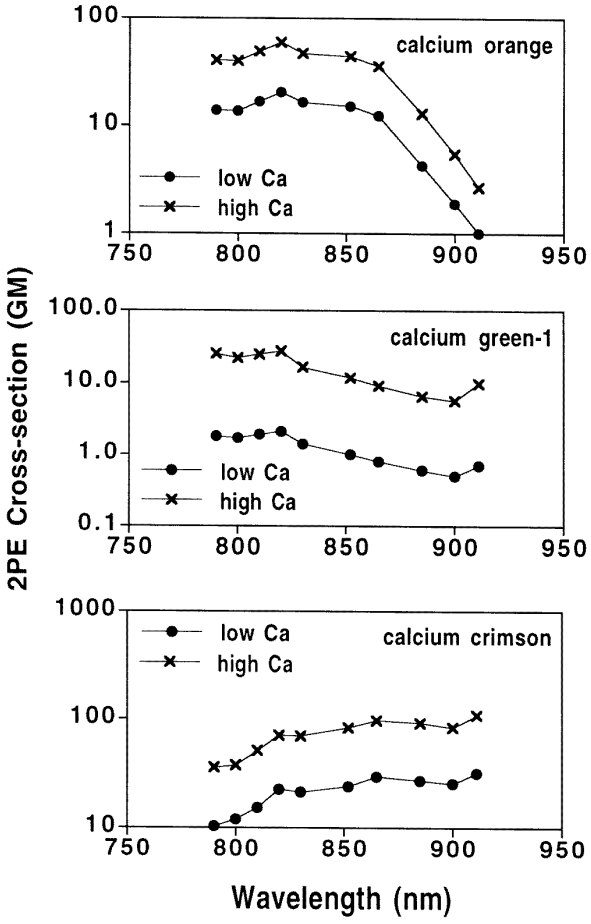

Figure 3. TPE spectra of Ca^{2+} indicators. The TPE spectra are identical for the free and Ca^{2+}-bound forms of Ca-Crimson, Ca-Orange and Ca-Green-1.

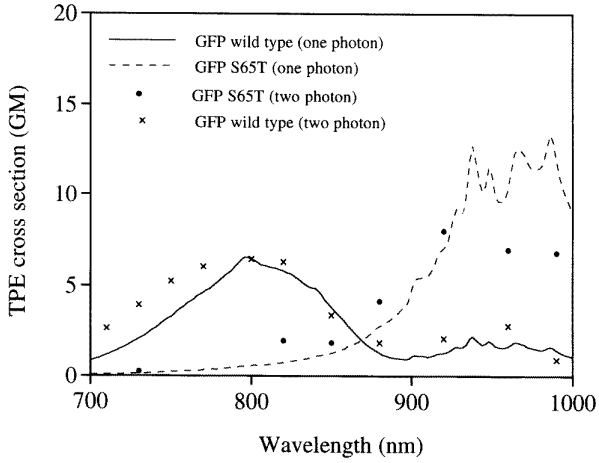

Figure 4. Two-photon action cross sections of GFPs. The *y*-axis values represent two-photon action cross sections for GFPs. For the single-photon results, the *x*-axis values represent twice the single-photon transition wavelengths and the *y*-axis values are arbitrarily scaled. GFPs are provided by George Patterson and David W Piston, Vanderbilt University.

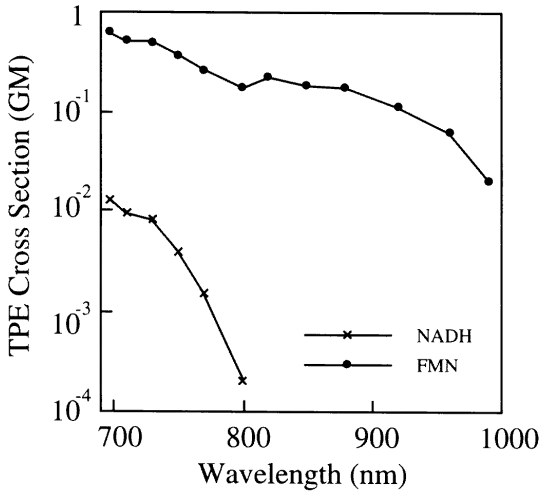

Figure 5. Two-photon action cross sections of the native fluorophores NADH and FMN. NADH and FMN are purchased from Sigma. Note that the *y*-axis is in logarithmic scale.

Two-photon-excited cellular autofluorescence from intrinsic chromophores such as NAD(P)H has been used to study the cellular metabolic state (Piston *et al* 1995). Photodamage of cells can also be detected by monitoring autofluorescence changes. However, for most fluorescence imaging applications, autofluorescence background is undesirable as it limits the detection sensitivity for fluorescent probes. Thus, knowledge of the two-photon excitation spectra of NADH and flavins should help to optimize two-photon-excited fluorescence imaging and may also provide insight into the photodamage mechanisms of living biological preparations in the near infrared (Konig *et al* 1995). We report in figure 5 measurements of the two-photon excitation spectra of NADH and FMN. Results for NADPH are nearly identical to NADH. The two-photon excitation spectrum of FAD is similar to FMN, although the action cross sections of FAD are approximately 9 times smaller than FMN (presumably due to quenching of fluorescence by the adenine).

One general feature conserved in all measured two-photon excitation spectra is that the two-photon excitation peak absorption wavelengths never appear red shifted (but are frequently blue shifted) relative to twice the single-photon absorption peaks. For example, large blue shifts were observed for rhodamine B, DiI, fluorescein, and several Ca^{2+} indicators (figures 1 and 2). Although these interesting spectral features still are not understood quantitatively, there are several desirable consequences of such significant blue shifts. First, the resolution of 2PLSM using these fluorophores is considerably higher than predicted by assuming two-photon excitation peak

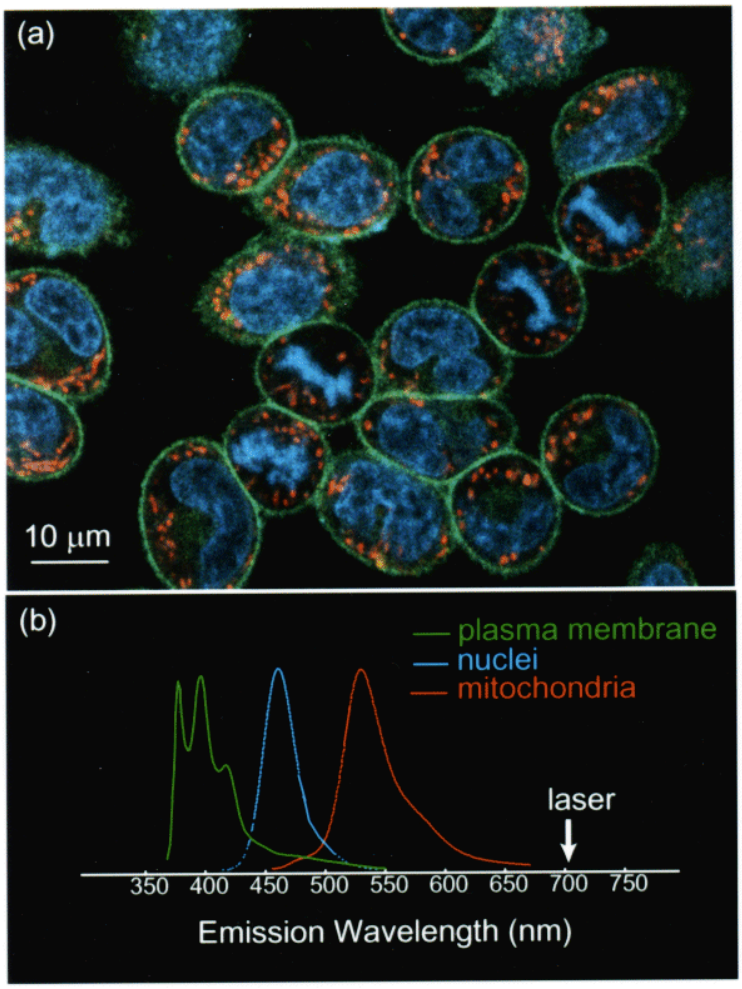

Figure 6. (Top) Three-color staining of plasma membrane, nuclei, and mitochondria in rat basophilic leukemia (RBL-2H3) cells visualized with two-photon illumination. The cells were incubated with three different stains—a plasma membrane label (pyrene lysophosphatidylcholine), a nuclear stain (DAPI) and a mitochondrial stain (Rhodamine 123). The image was obtained using a modified BioRad MRC-600 confocal microscope to scan the excitation beam (705 nm, ∼ 120 fs pulsewidth, 80 MHz repetition rate, ∼ 5 mW at the sample) through a 40×/1.3 NA oil immersion objective. Epi-fluorescence was collected using non-descanned external detection into three channels: 400 nm, 30 nm FWHM (pyrene fluorescence—green); 440 nm, 50 nm FWHM (DAPI fluorescence—blue) and 530 nm, 30 nm FWHM (Rhodamine 123 fluorescence—red). The insert at the bottom shows the excitation laser wavelength and the approximate emission spectra of the dyes used (color coded as in the image).

wavelengths at twice the single-photon absorption peak wavelengths. Second, the blue shifts allow conveniently available mode-locked laser sources to excite popular dyes as indicated in figures 1 and 2. Finally conventional dyes possessing differing single-photon absorption spectra can be excited by two-photon excitation at a single wavelength. This capability, combined with the large spectral separation between the excitation light and the fluorescence light, greatly simplifies experiments requiring multiple fluorophores. We show in figure 6 simultaneous excitation of rhodamine 123, DAPI and pyrene using a single 705 nm illumination line.

Fluorescence resonance energy transfer (FRET) is a powerful tool for measuring intermolecular distances (Stryer 1978). The applicability of FRET depends on the overlap of fluorescence emission and excitation spectra of the donor and acceptor. We have found no significant fluorescence emission spectra difference between single- and two-photon excitation for the fluorophores investigated in our experiments (Xu and Webb 1996). Knowledge of the two-photon excitation spectra also provides new capabilities by combining FRET with two-photon excitation. For example, the optimum excitation wavelength of two-photon excitation FRET using fluorescein and rhodamine is ∼ 920 nm (figure 2). Significantly better choices of donor and acceptor in two-photon excitation FRET would be fluorescein and DiI (or Cy-3, the two-photon excitation spectrum of which is similar to that of DiI) when excited at ∼ 790 nm, where the fluorescein two-photon excitation cross-section is approximately 200 times larger than DiI.

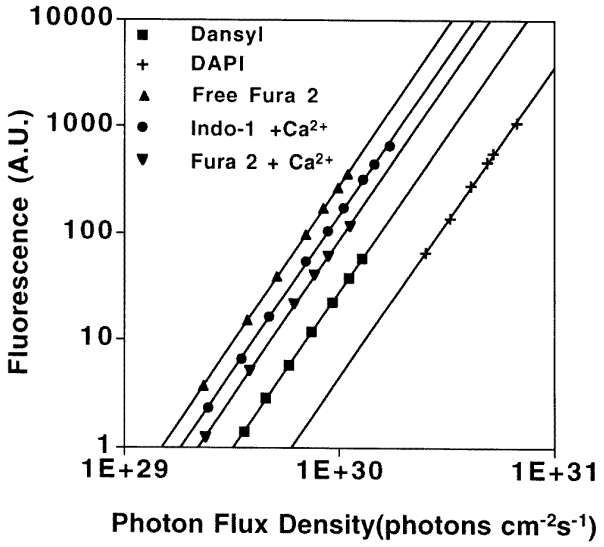

Figure 7. Logarithmic plots of the dependence of relative three-photon-excited fluorescence on the peak incident photon flux density at the geometric focal points in five fluorophore solutions. The concentrations are 10^{-4} M and the excitation wavelength is 1.0 μm. The excitation pulse-width is about 110 fs (assuming sech^2 pulse shape). The solid lines represent the best power law fits to the experimental data with slopes of 2.92, 2.96, 2.93, 2.94 and 2.91 for dansyl, free fura-2, indo-1+Ca, fura-2+Ca and DAPI, respectively. The estimated uncertainties in the slopes are $\pm$ 3%.

3. Three-photon excitation

Very recently, unexpectedly large three-photon absorption cross-sections (with $\sigma_3 \sim 10^{-75}$ cm^6 s^2) have been reported (Davey *et al* 1995, He *et al* 1995). The discoveries of such large cross-sections are promising. We have observed and measured three-photon-excited fluorescence from UV fluorophores such as Ca^{2+} indicator fura-2 and indo-1, DNA stain DAPI, and the fluorescent reagent dansyl hydrazine by excitation at $\lambda \sim 1.0$ μm (figure 7). These fluorophores are normally excited at approximately 330 nm to 360 nm and exhibit no linear absorptions at the single-photon energy or the two-photon energy of 1.0 μm radiation. The three-photon energy of the 1.0 μm radiation falls into the UV absorption band, and therefore three-photon fluorescence is expected. The approximate three-photon cross-sections (σ_3) are listed in table 1. For a comparison, the corresponding single- and two-photon cross-sections are also given. The slopes obtained in figure 7 are slightly less than 3.0. We currently do not understand the significance of such small deviations because the estimated contributions resulting from two-photon excitation at 1.0 μm are negligible.

To investigate the photophysics of three-photon excitation of fluorophores, we have measured several three-photon excitation spectra ($\sigma_3(\lambda)$) from 960 to 1050 nm for comparison with single-photon excitation spectra (figure 8). The qualitative agreement shown in figure 8 suggests that these three-photon excitation spectra parallel the corresponding single-photon excitation spectra as expected because the same initial excited states can be reached via single- or three-photon excitation without violating any selection rules. Three-photon-excited fluorescence emission spectra of several fluorophores were also measured. We found no difference between two- and three-photon-excited fluorescence, which indicates that the fluorescence is emitted from the same state regardless of the excitation mode. Previously we have observed no difference between the emission spectra of single- and two-photon-excited fluorescence (Xu and Webb 1996, Xu *et al* 1995) suggesting that quite generally the same fluorescent states are reached by nonlinear and linear excitation.

To demonstrate the imaging capability of three-photon-excited fluorescence, chromosomes in a rat basophilic leukemia (RBL) cell stained with DAPI were imaged in a laser scanning microscope at $\sim$ 1.0 μm (figure 9), and compared with two-photon microscopy which also provides excellent (virtually indistinguishable) images in this application (Williams *et al* 1994). Because the quantum efficiency of our PMT with a bialkali cathode is extremely low at 1.0 μm, no emission filter is required to block the scattered excitation light. A blank control performed with unstained RBL cells under identical experimental conditions showed a negligible amount of autofluorescence. The longer wavelengths required for three-photon excitation should slightly degrade the resolution; for the imaging conditions of figure 9, the calculated FWHM of the fluorescence distribution of a point source resulting from three-photon excitation at 1.05 μm is $\sim$ 0.24 μm in the focal plane and 0.73 μm along the

Table 1. Single-, two- and three-photon excitation cross-sections (σ). Cross-sections were measured in 10^{-4} M solution. η is the fluorescence quantum efficiency. We have assumed that two- and three-photon fluorescence quantum efficiency are the same. The estimated uncertainties are 30% for the two-photon cross-sections and about a factor of 3 for the three-photon cross-sections.

	σ_1 (at λ nm) 10^{-16} cm^2	$\eta * \sigma_2$ (at 700 nm) 10^{-50} cm^4 s/photon	$\eta * \sigma_3$ (at 1.0μm) 10^{-83} cm^6 (s/photon)^2
DAPI[a]	1.3 (345 nm)	0.16	0.25
dansyl	0.17 (336 nm)	1	0.3
fura-2 with Ca^{2+}	1.2 (335 nm)	12	30
fura-2 free	1.0 (362 nm)	11	20
indo-1 with Ca^{2+}	1.3 (340 nm)	1.5	6
indo-1 free	1.3 (345 nm)	3.5	2

[a] DAPI not bound to DNA. The fluorescence quantum efficiency of DAPI is expected to go up by 20-fold upon binding to DNA. (Molecular Probes Handbook 1992–94, R P Haugland (ed), p 222.)

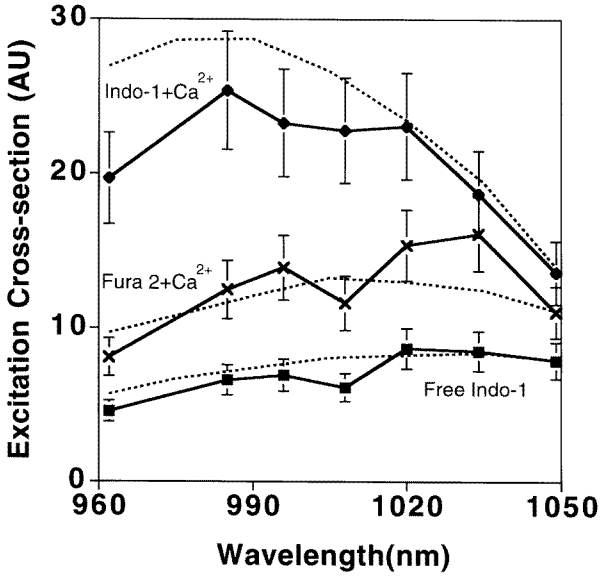

Figure 8. Comparison of single-photon (dashed lines) and three-photon (solid lines) fluorescence excitation of indo-1 and fura-2. For the single-photon results, the x-axis values represent 3 times the single-photon transition wavelengths. The single-photon results are normalized to their corresponding three-photon data at 1050 nm.

optical axis, while the corresponding numbers for two-photon excitation at 700 nm are ~ 0.2 μm and ~ 0.6 μm (Sheppard and Gu 1990, Hell and Stelzer 1992). However, there is a compensating image enhancement because the signal-to-background ratio (S/B) (Sandison and Webb 1994) of a three-photon microscope is theoretically equivalent to application of an ideal confocal spatial filter in 2PLSM. In a uniform fluorescent sample, for example, $\sim$ 24% of total generated fluorescence is from a volume that is within the FWHM of the fluorescence distribution in two-photon excitation, while the corresponding figure for three-photon excitation is $\sim$ 31% . When taking the signal-to-background ratio into account, the effective resolution of two- and three-photon fluorescence microscopy should be comparable.

Our application of three-photon-excited fluorescence to laser scanning microscopy was originally designed to detect intrinsic chromophores, such as amino acids, proteins and neurotransmitters, using relatively benign excitation wavelengths accessible with commercially available near-IR lasers (Maiti *et al* 1996a). In addition to background interference, photodamage to living cells by deep UV excitation has previously limited the use of imaging of native fluorescence. Our measured fluorescence excitation cross sections of tryptophan and serotonin predicted detectable two- and three-photon fluorescence from large secretory vesicles (Maiti *et al* 1996a). Combined with the inherent three-dimensional resolution of multiphoton excitation using highly focused femtosecond laser pulses and the relative transparency of biological materials to these longer wavelengths, these results suggest new imaging possibilities utilizing the native UV-excitable fluorescence of cellular materials. In a preliminary study, secretary granules in RBL cells have been successfully imaged using three-photon-excited fluorescence of serotonin (Maiti *et al* 1996b).

4. Discussion

The applicability of nonlinear microscopy depends crucially on the two- and three-photon fluorescence excitation cross-sections of various fluorophores and biomolecules. A simple estimation of MPE cross-sections can be obtained using the appropriate order perturbation theory (Faisal 1987). Intuitively, these multiphoton processes require two or more photons to interact *simultaneously* with the molecule. The 'cross-sectional' area (A) of a molecule can be estimated by its dipole transition length (typically $A \approx 10^{-16}$ to 10^{-17} cm^2 for a transition length of 10^{-8} to 10^{-9} cm). The time scale for photon coincidence is determined by the lifetimes of the virtual intermediate states $\Delta\tau \approx 10^{-16}$ s (estimated from the uncertainty principle). Hence, the expected two-photon excitation cross-sections (σ_2) are approximately 10^{-49} cm^4 s/photon (i.e., $A^2\Delta\tau$). Correspondingly, the three-photon excitation cross-sections are expected to be $\sigma_3 \sim 10^{-82}$ cm^6 (s/photon)^2 (i.e., $A^3\Delta\tau^2$). Table 1 and figure 1 show that these estimates are in qualitative agreement with our experimental data.

The maximum fluorescence output available for image formation is obtained using ultrashort ($\sim$ 100 fs) pulsed excitation. However, fluorescence saturates at the limit of one transition per pulse per fluorophore. For an n-photon process, fluorescence output per excitation pulse, neglecting ground state depletion, is proportional to $\alpha \equiv \sigma_n I_{\text{peak}}^n \tau$, where I_{peak} is the peak intensity at the geometric focal point (Xu and Webb 1996) σ_n is the n-photon cross section and τ is the pulse width. When $\alpha << 1$, α rigorously represents the excitation probability per molecule per pulse. For a square pulse in time, saturation occurs when $\alpha \approx 1$. With a high numerical aperture (NA $= 1.3$) objective lens and a mode-locked Ti:sapphire laser providing 100 fs pulses at 80 MHz repetition rate and 1.0 μm excitation wavelength, the estimated saturation powers for two-, three- and four-photon processes are, respectively, $\sim$ 30 mW, $\sim$ 150 mW, and $\sim$ 300 mW using the excitation cross-sections estimated above (Xu *et al* 1996a). Although these incident power levels are easily available from femtosecond laser sources such as the mode-locked Ti:sapphire laser, solvent dielectric breakdown may occur before reaching saturation in three- and four-photon excitation.

The three-dimensional (3-D) resolution of two-photon laser scanning microscopy results from the quadratic power dependence of the two-photon-excited fluorescence (Denk *et al* 1990). However, such a quadratic relation no longer

Figure 9. One section through a dividing rat basophilic leukemia (RBL) cell stained with DAPI. The image is $\sim$ 15 by 20 μm, and is a Kalman average of 4 scans (1 second acquisition time per frame). The image was collected as in figure 5, except that excitation wavelength was 1000 nm (120 fs pulsewidth) and only one collection channel was used without an emission filter. The average excitation power at the sample was approximately 9.5 mW, which corresponds to a peak photon flux density at the geometric focal point of approximately 3×10^{30} photons $\mathrm{cm}^{-2}\ \mathrm{s}^{-1}$. Figure(7) shows the power cubic dependence of DAPI fluorescence at this intensity region.

holds under the saturation condition (Xu 1996). Thus, the spatial localization of two-photon excitation begins to degrade when $\alpha \sim 1$ and will become nonlocalized when $\alpha >> 1$. In order to quantitatively study the resolution at various excitation intensity levels, we present the radial and axial full width half maximum (FWHM) of the two-photon-excited fluorescence distribution as a function of the saturation parameter α (figure 10) (Xu 1996). More detailed analysis of saturation under MPE can be found in Xu (1996). It is apparent that the axial resolution degrades significantly faster than does the radial resolution. Intuitively, this can be understood because the fluorescence power decreases much faster in the radial direction (exponentially) than in the axial direction (power law). In the extreme hypothetical case where the edge of the fluorescence distribution is infinitely sharp, (i.e., a

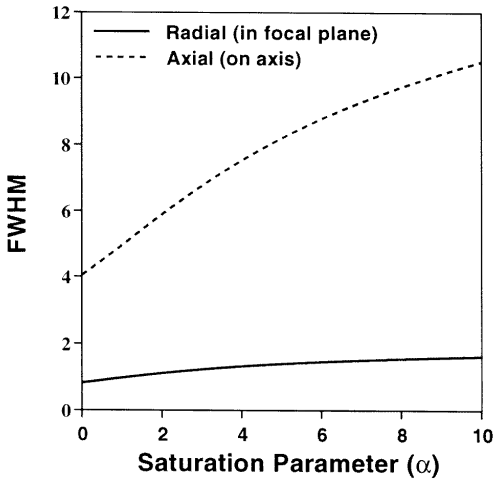

Figure 10. Effects of saturation of excitation on image resolution. FWHM values of the two-photon-excited fluorescence distribution generated by a Gaussian–Lorentzian excitation beam as a function of the saturation parameter. FWHM values are normalized to the $(1/e^2)$ radius of the Gaussian beam waist w_0. The excitation wavelength (λ) is set to be $\lambda = w_0$. We have assumed that the time between adjacent pulses is much greater than the fluorescence life time of the fluorophore.

'tophat' distribution), there should be no resolution decrease regardless of the saturation level.

To increase the probability of simultaneous multiphoton incidence, pulsed lasers with high peak intensity are generally used as the excitation source. For example, a mode-locked Ti:sapphire laser with 100 MHz repetition rate and 100 fs pulses provides enhancement factors of 10^5 and 10^{10} for two- and three-photon excitation, respectively, when compared with a cw laser. However, such a high degree of temporal focus, combined with the tight spatial focus (typically $< 1\ \mu m^2$), results a peak intensity that is many orders of magnitude higher than in normal single-photon excitation. Although peak intensities at the focal point are generally less than 3×10^{11} Wcm^2 in routine 2PLSM, other applications can necessitate use of far higher intensities. Uncaging of biological effector molecules in three-dimensionally specified volumes, for example, can require as much as 10^{12} Wcm^2. Note that intensities used in single-photon excitation are typically less than 10^6 Wcm^2. The high peak intensities used in MPE opens a range of new laser–matter interactions that have previously been neglected in single-photon excitation. Although dielectric breakdown of pure water is not expected until peak intensities above 10^{13} Wcm^2 in the femtosecond region (Smith 1978, Stuart *et al* 1995, Du *et al* 1994) the photophysical responses of cellular materials and biological buffers to very intense radiation fields are yet to be explored in detail. In fact, knowledge of high intensity damage phenomena is scarce even in non-biological systems when 100 femtosecond pulsed excitation is used.

Laser–matter interactions are strongly intensity dependent. At relatively low intensities (generally $< 10^{12}$ Wcm^2), linear and perturbative nonlinear phenomena dominate. At intensities significantly above 10^{12} Wcm^2, nonperturbative nonlinear phenomena become important. It is worth noting that intensities required for two-photon uncaging and three- or even four-photon imaging may lie between the perturbative and nonperturbative region, an issue can cause considerable complications in both the theoretical and experimental investigations of MPE. The relative contributions of various order processes depends on the incident intensity. As the intensity increases, so does the relative contribution of the higher-order processes. Thus, mechanisms of photobleaching and photodamage can change fundamentally at high intensities. Higher-order processes may contribute significantly at the high-intensity region, a phenomenon that has been observed in our measurements of serotonin photobleaching (Shear *et al* 1996). Experiments on the characterization of these fundamental processes are currently underway in our laboratory. The possibility of higher-order excitation complicates quantitative experiments on possible photodamage during two-photon imaging.

5. Conclusion

We have reported two-photon fluorescence excitation spectra of the most common biological fluorophores in the tuning range of a mode-locked Ti:sapphire laser. These spectra show that nonlinear fluorescence microscopy based on two-photon excitation works well with most existing fluorophores and conveniently available laser sources. We have also measured three-photon fluorescence excitation cross-sections and have shown the feasibility of three-photon fluorescence microscopy. Although three-photon microscopy requires 5–10 times higher incident power than comparable two-photon laser scanning microscopy to obtain comparable fluorescence excitation rate (under conditions discussed in section 4), it does provide alternative wavelength windows to probe biological specimens. The significance of such a wavelength option depends on the laser availability and the photodamage mechanism for various applications. Unfortunately, the wavelength dependence of the amount of photodamage to living cells is largely unknown and may vary greatly for various applications. Various research groups are currently working towards elucidating the photodamage mechanisms. With the aid of such information and the knowledge of the nonlinear absorption spectra (such as reported here), it is conceivable that the optimum excitation mode (two- or three-photon) can be determined for each individual system in the future, making three-photon excitation a useful complement to the existing 2PLSM.

Acknowledgment

This work was carried out in the Developmental Resource for Biophysical Imaging and Opto-electronics with funding by NSF (DIR8800278), NIH(RR04224) and NIH(RR07719). The authors acknowledge fruitful discussions with J Mertz and J Guild.

References

Birge R R 1983 *Ultrasensitive Laser Spectroscopy* ed D S Kliger (New York: Academic) pp 109–74

Chalfie M, Tu Y, Euskirchen G, Ward W W and Prasher D C 1994 Green fluorescence protein as a marker for gene expression *Science* **263** 802–5

Cormack B P, Valdivia R H and Falkow S 1996 FACS-optimized mutants of the green fluorescent protein (GFP) *Gene* **173** 33–8

Cubitt A B, Heim R, Adams S R, Boyd A E, Gross L A and Tsien R Y 1995 Understanding, improving and using fluorescent proteins *Trends Biol. Sci.* **20** 448–55

Davey A P, Bourdin E, Henari F and Blau W 1995 Three-photon induced fluorescence from a conjugated organic polymer for infrared frequency upconversion *Appl. Phys. Lett.* **67** 884–85

Denk W, Piston D W and Webb W W 1995 *The Handbook of Confocal Microscopy* ed J Pawley (New York: Plenum) pp 445–58

Denk W, Strickler J H and Webb W W 1990 Two-photon laser scanning fluorescence microscopy *Science* **248** 73–6

Du D, Liu X, Squier K J and Mourou G 1994 Laser-induced breakdown by impact ionization in SiO(2) with pulsewidths from 7 ns to 150 fs *Appl. Phys. Lett.* **64** 3071–3

Faisal F H M 1987 *Theory of Multiphoton Processes* (New York: Plenum)

Göppert-Mayer M 1931 Über Elementarakte mit zwei Quantensprüngen *Ann. Phys.* **9** 273–95

Gryczynski I, Szmacinski H and Lakowicz J R 1995a On the possibility of calcium imaging using indo-1 with three-photon excitation *Photochem. Photobiol.* **62** 804–8

——1995b Three-photon induced fluorescence of 2,5-diphenyloxazole with a femtosecond Ti:sapphire laser *Chem. Phys. Lett.* **245** 30–5

He G S, Bhawalkar J D and Prasad P N 1995 Three-photon-absorption-induced fluorescence and optical limiting effects in an organic compound *Opt. Lett.* **20** 1524–6

Hell S W, Bahlmann K, Schrader M A S H M, Gryczynski I and Lakowicz J R 1996 Three-photon excitation in fluorescence microscopy *J. Biomed. Opt.* **1** 71–4

Hell S and Stelzer E H K 1992 Fundamental improvement of resolution with a 4Pi-confocal fluorescence microscope using two-photon excitation *Opt. Commun.* **93** 277–82

Hermann J P and Ducuing J 1972 Absolute measurement of two-photon cross-sections *Phys. Rev.* A **5** 2557–68

Kaiser W and Garrett C G B 1961 Two-photon excitation in CaF_2:Eu^{2+} *Phys. Rev. Lett.* **7** 229

Konig K, Liu Y, Sonek G J, Berns M and Tromberg B J 1995 Autofluorescence spectroscopy of optically trapped cells *Photochem. Photobiol.* **62** 830–5

Maiti S, Shear J B and Webb W W 1996a Multiphoton excitation of amino acids and neurotransmitters: a prognosis for *in situ* detection *Biophys. J.* **70** A210

Maiti S, Shear J B, Zipfel W, Williams R M and Webb W W 1996b *Science* submitted

McClain W M and Harris R A 1977 *Excited States* ed E C Lim (New York: Academic) pp 1–56

Niswender K D, Blackman S M, Rohde L, Magnuson M A and Piston D W 1995 Quantitative imaging of green fluorescent protein in cultured cells: comparison of microscopis techniques use in fusion proteins and detetction limits *J. Microsc.* **180** 109–16

Piston D W, Masters B R and Webb W W 1995 Three dimensionally resolved NAD(P)H cellular metabolic redox imaging of the *in situ* cornea with two-photon excitation laser scanning microscopy *J. Microsc.* **178** 20–7

Potter S M, Wang C M, Garrity P A and Fraser S E 1996 Intravital imaging of green fluorescent protein using two-photon laser-scanning microscopy *Gene* **173** 25–31

Sandison D R and Webb W W 1994 Background rejection and signal-to-noise optimization in confocal and alternative fluorescence microscopy *Appl. Opt.* **33** 603–15

Shear J B, Xu C and Webb W W 1996 *Photochem. Photobiol.* in press

Sheik-Bahae M, Said A A, Wei T-H, Hagan D and Van Stryland E W 1990 Sensitive measurement of optical nonlinearities using a single beam *IEEE J. Quantum Electron.* **26** 760–9

Sheppard C J R and Gu M 1990 Image formation in two-photon fluorescence microscopy *Optik* **86** 104

Smith W L 1978 Laser-induced breakdown in optical materials *Opt. Eng.* **17** 489–503

Stryer L 1978 Fluorescence energy transfer as a spectroscopic ruler *Ann. Rev. Biochem.* **47** 819–46

Stuart B C, Feit M D, Rubenchik A M, Shore B W and Perry M D 1995 Laser-induced damage in dielectrics with nanosecond to subpicosecond pulses *Phys. Rev. Lett.* **74** 2248–51

Svoboda K, Tank D W, and Denk W 1996 Direct measurement of coupling between dendritic spines and shafts *Science* **272** 716–19

Swofford R and McClain W M 1975 The effect of spatial and temporal laser beam characteristics on two-photon absorption *Chem. Phys. Lett.* **34** 455–60

Twarowski A J and Kliger D S 1977 Multiphoton absorption spectra using thermal blooming *Chem. Phys.* **20** 259

Williams R M, Piston D W and Webb W W 1994 Two-photon molecular excitation provides intrinsic 3-dimensional resolution for laser-based microscopy and microphotochemistry *Faseb Journal* **8** 804–13

Wokosin D L, Centonze V E, Crittenden S and White J G 1995 Three-photon excitation of blue-emitting fluorophores by laser scanning microscopy *Molecular Biology of the Cell* **6** 113a (unrefereed conference abstract)

Xu C 1996 *PhD thesis* Cornell University

Xu C, Guild J, Webb W W and Denk W 1995 Determination of absolute two-photon excitation cross-sections by *in situ* second-order autocorrelation *Opt. Lett.* **20** 2372–4

Xu C and Webb W W 1996 Measurement of two-photon excitation cross-sections of molecular fluorophores with data from 690 nm to 1050 nm *J. Opt. Soc. Am.* B **13** 481–91

Xu C, Zipfel W, Shear J B, Williams R M and Webb W W 1996a Multiphoton fluorescence excitation: new spectral windows for biological nonlinear microscopy *Proc. Nat. Acad. Sci. USA* **93** 10763–8

Xu C, Zipfel W and Webb W W 1996b Three-photon-excited fluorescence and applications in nonlinear microscopy *Biophys. J.* **70** A429

Yuste R and Denk W 1995 Dendritic spines as basic function units of neuronal integration *Nature* **375** 682–4